

Supporting information

First-principles design of bifunctional oxygen reduction and evolution catalysts through bimetallic centers in metal-organic frameworks

Peng Zhang^{1,3,4}, Xuejing Yang¹, Wang Gao², Xiuli Hou¹, Jianli Mi¹, Lei Liu¹, Jun
Huang^{*,4}, Mingdong Dong^{*,5}, Catherine Stampfl^{*,3}

¹ *Institute for Advanced Materials, School of Materials Science and Engineering,
Jiangsu University, Zhenjiang 212013, China*

² *School of Materials Science and Engineering, Jilin University, Changchun 130022,
China*

³ *School of Physics, The University of Sydney, Sydney, New South Wales 2006,
Australia*

⁴ *Laboratory for Catalysis Engineering, School of Chemical and Biomolecular
Engineering, The University of Sydney, New South Wales 2006, Australia*

⁵ *Interdisciplinary Nanoscience Center (iNANO), Aarhus University, Aarhus DK-
8000, Denmark*

**E-mail: jun.huang@sydney.edu.au, dong@inano.au.dk,*

catherine.stampfl@sydney.edu.au

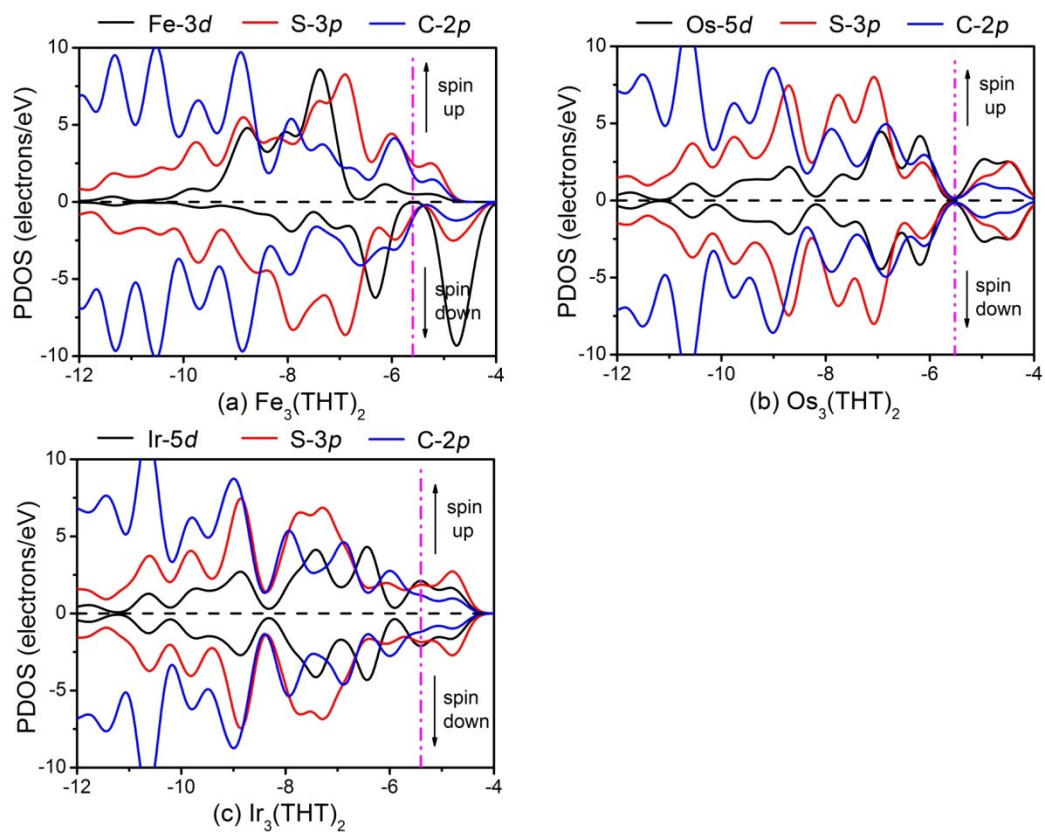


Fig. S1. Partial density of states (PDOS) of (a) $\text{Fe}_3(\text{THT})_2$, (b) $\text{Os}_3(\text{THT})_2$, and (c)

$\text{Ir}_3(\text{THT})_2$.

Table S1. Adsorption energy (E_{ad}) values of ORR intermediates and d-band center of $M_3(\text{THT})_2$ nanosheets. All results are in the unit of eV. The corresponding adsorption structures are shown in Fig. S2.

E_{ad}	OOH	O	OH	ϵ_d
Fe	1.36	3.92	2.51	-1.23
Ru	1.76	4.86	2.35	-1.88
Os	1.96	5.59	3.18	-2.05
Co	0.87	3.77	2.07	-1.56
Rh	0.96	4.03	2.08	-2.13
Ir	0.95	3.91	2.18	-2.59
Ni	0.51	3.68	1.93	-1.88
Pd	0.64	3.74	2.05	-2.62
Pt	0.49	3.63	1.90	-3.01
Fe/Fe ₂ Co	1.37	3.95	2.52	-1.14
Co/Fe ₂ Co	0.89	3.56	2.07	-1.56
Fe/FeCo ₂	1.37	3.98	2.58	-1.15
Co/FeCo ₂	0.86	3.75	2.02	-1.57

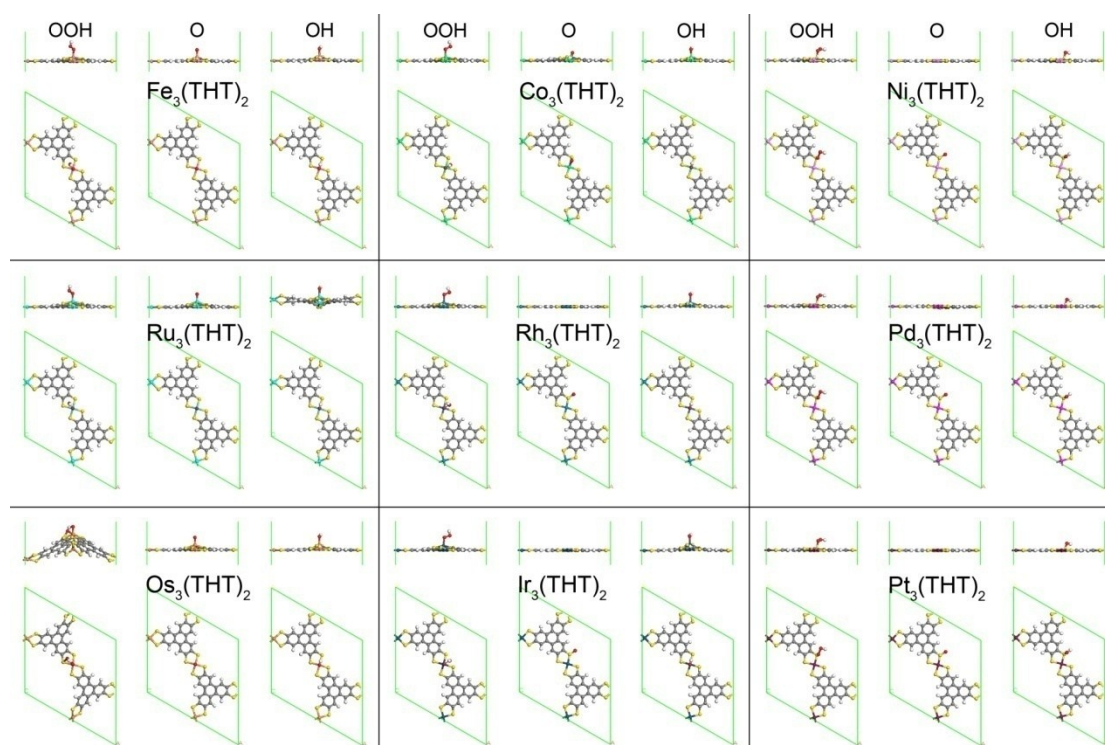


Fig. S2. Favorable adsorption structures of ORR intermediates on single-metal $M_3(\text{THT})_2$ nanosheets.

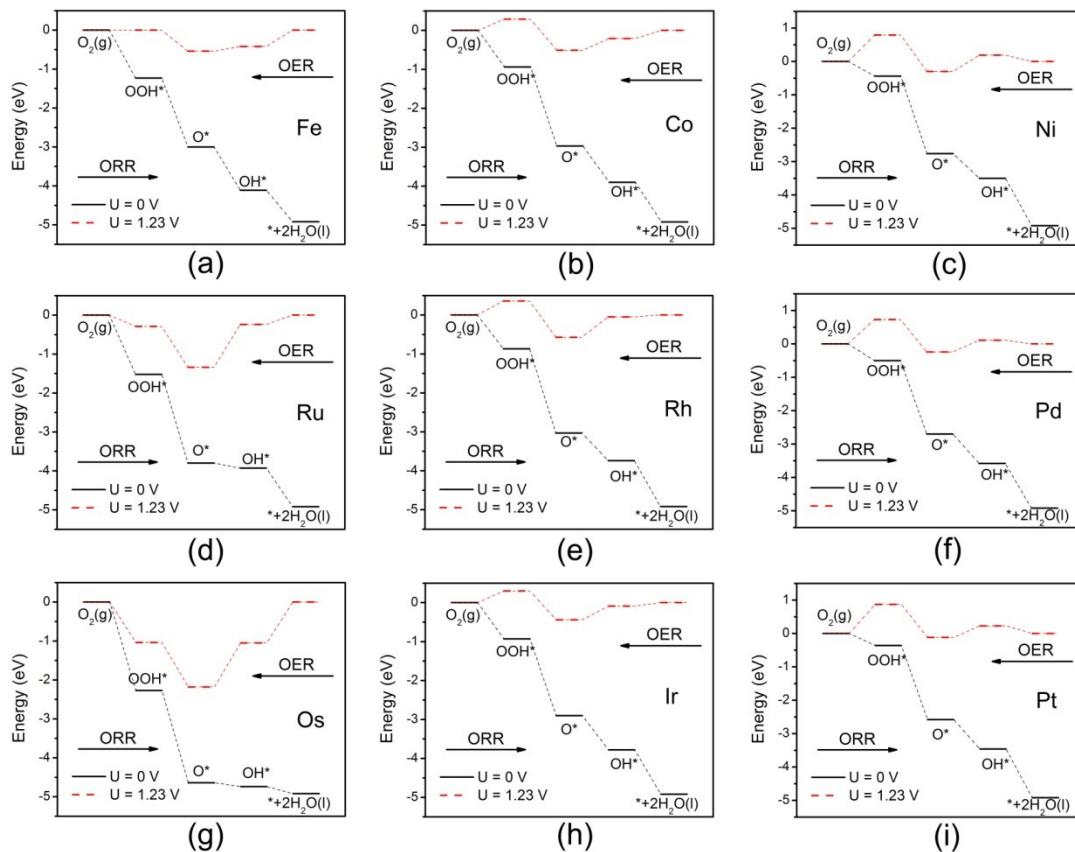


Fig. S3. Schematic free energy diagrams for ORR/OER on single-metal $M_3(\text{THT})_2$ nanosheets.

Table S2. Mulliken charge analysis for $\text{Fe}_3(\text{THT})_2$, $\text{Co}_3(\text{THT})_2$, $\text{Fe}_2\text{Co}(\text{THT})_2$ and $\text{FeCo}_2(\text{THT})_2$ in units of e .

	Fe	S-Fe ^a	Co	S-Co ^a
$\text{Fe}_3(\text{THT})_2$	0.425	-0.233		
$\text{Co}_3(\text{THT})_2$			0.147	-0.161
$\text{Fe}_2\text{Co}(\text{THT})_2$	0.424	-0.234	0.148	-0.161
$\text{FeCo}_2(\text{THT})_2$	0.419	-0.233	0.147	-0.161

^a S-Fe and S-Co indicate the S atoms bonded with Fe or Co atoms.

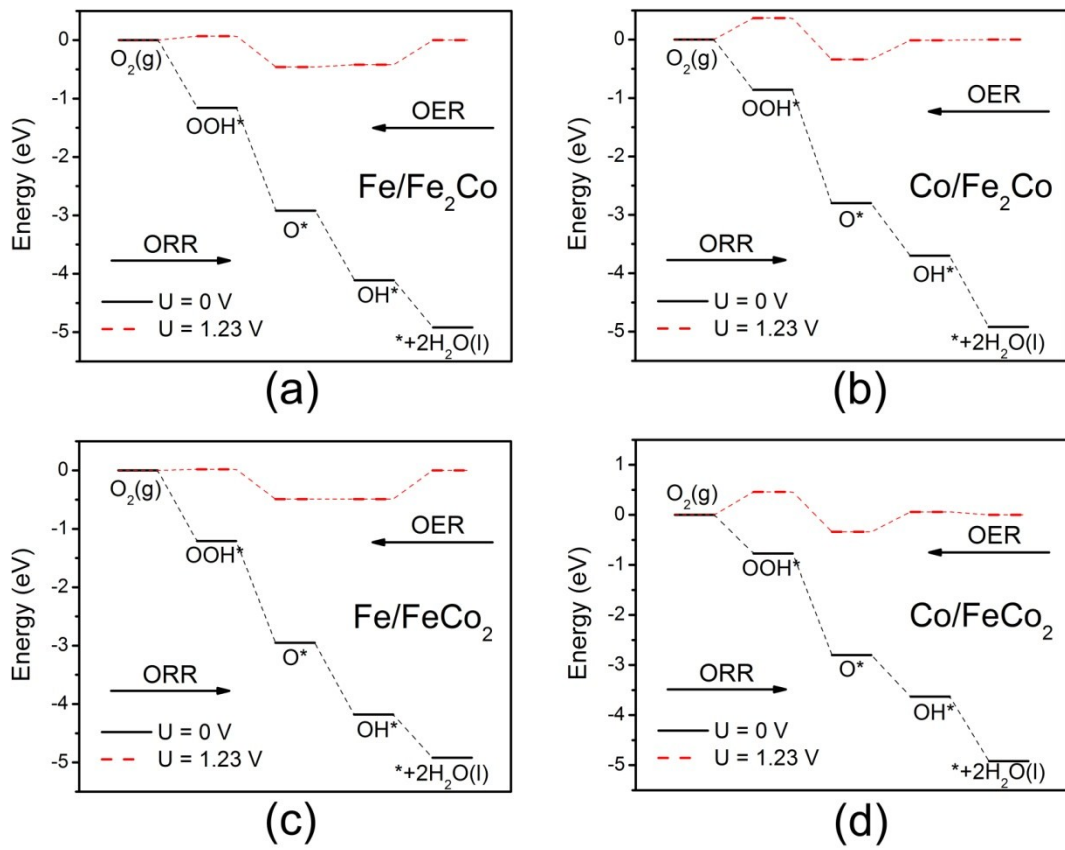


Fig. S4. Schematic free energy diagrams for ORR/OER on Fe_xCo_{3-x}(THT)₂

nanosheets.

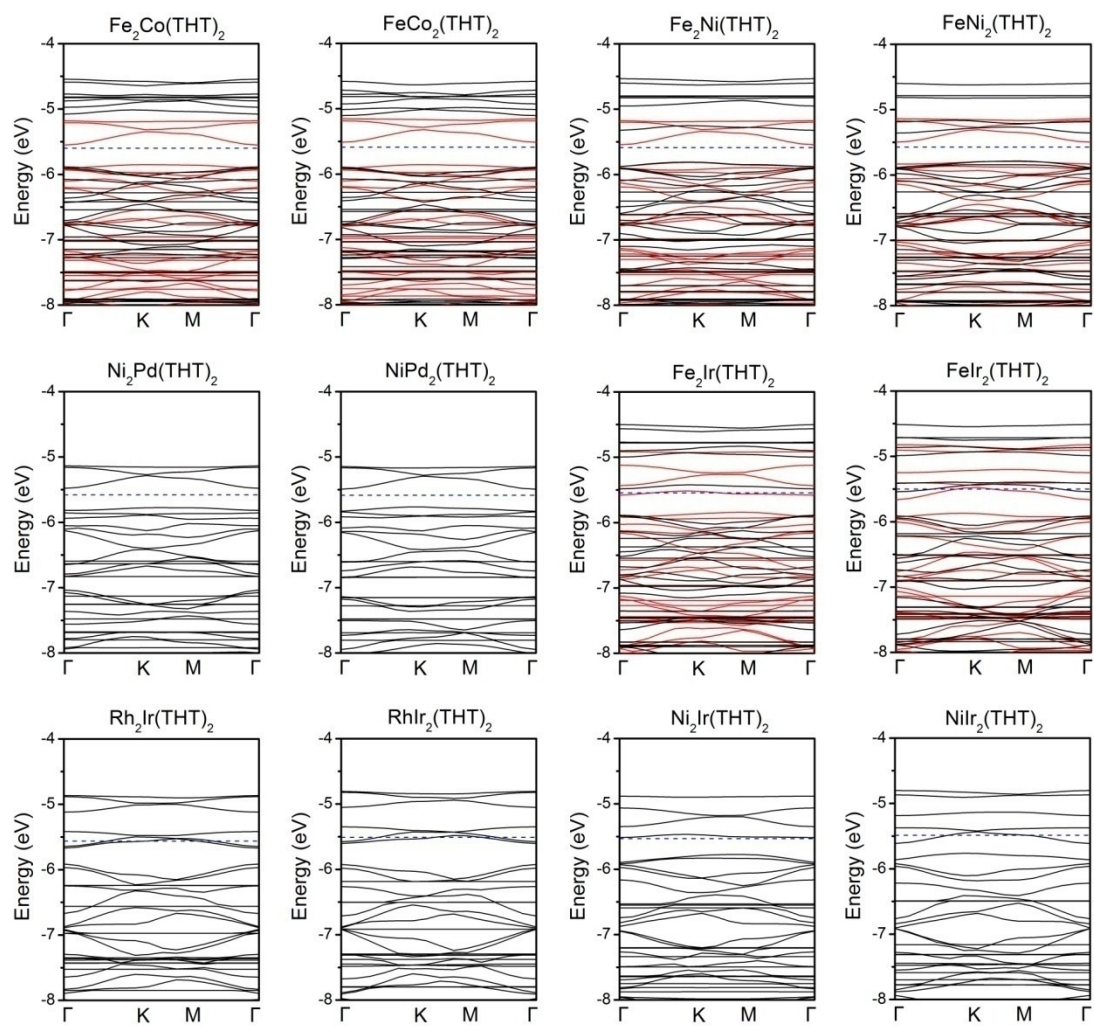


Fig. S5. The band structures of bi-metal $M_3(\text{THT})_2$ nanosheets.

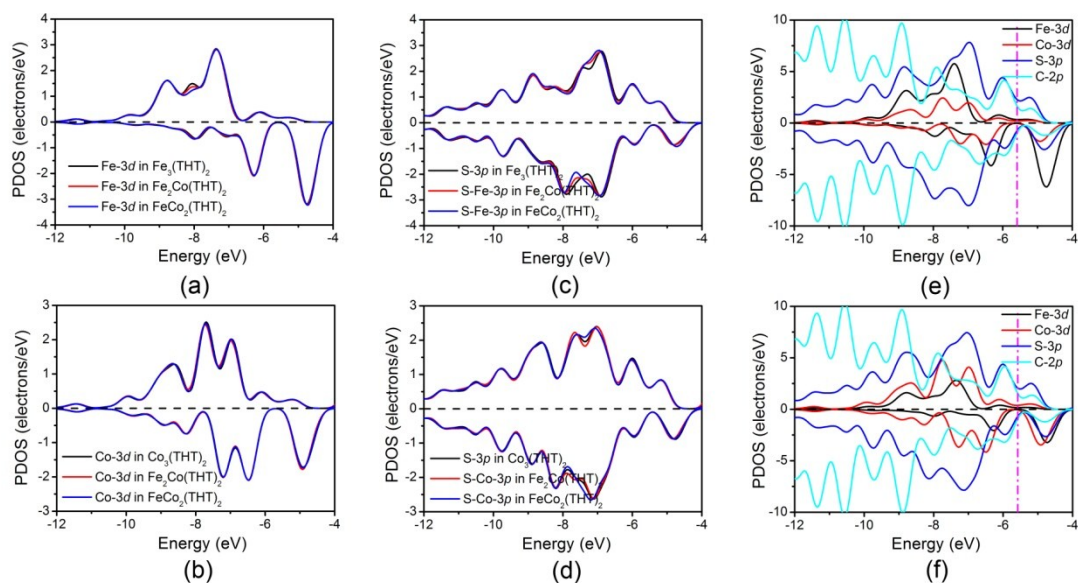


Fig. S6. Partial density of states (PDOS) of (a) Fe-3*d* in Fe₃(THT)₂, Fe₂Co(THT)₂, and FeCo₂(THT)₂, (b) Co-3*d* in Co₃(THT)₂, Fe₂Co(THT)₂, and FeCo₂(THT)₂, (c) S-3*p* of S atoms bonded with Fe atoms in Fe₃(THT)₂, Fe₂Co(THT)₂, and FeCo₂(THT)₂, (d) S-3*p* of S atoms bonded with Co atoms in Co₃(THT)₂, Fe₂Co(THT)₂, and FeCo₂(THT)₂, (e) Fe₂Co(THT)₂, and (f) FeCo₂(THT)₂.

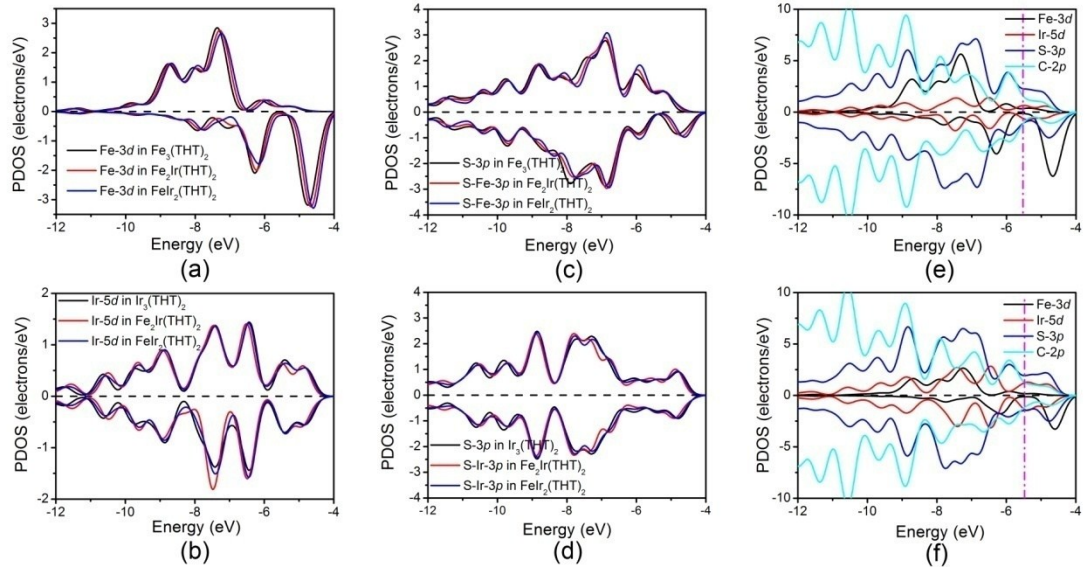


Fig. S7. Partial density of states (PDOS) of (a) Fe-3d in $\text{Fe}_3(\text{THT})_2$, $\text{Fe}_2\text{Ir}(\text{THT})_2$, and $\text{FeIr}_2(\text{THT})_2$, (b) Ir-5d in $\text{Ir}_3(\text{THT})_2$, $\text{Fe}_2\text{Ir}(\text{THT})_2$, and $\text{FeIr}_2(\text{THT})_2$, (c) S-3p of S atoms bonded with Fe atoms in $\text{Fe}_3(\text{THT})_2$, $\text{Fe}_2\text{Ir}(\text{THT})_2$, and $\text{FeIr}_2(\text{THT})_2$, (d) S-3p of S atoms bonded with Co atoms in $\text{Ir}_3(\text{THT})_2$, $\text{Fe}_2\text{Ir}(\text{THT})_2$, and $\text{FeIr}_2(\text{THT})_2$, (e) $\text{Fe}_2\text{Ir}(\text{THT})_2$, and (f) $\text{FeIr}_2(\text{THT})_2$.

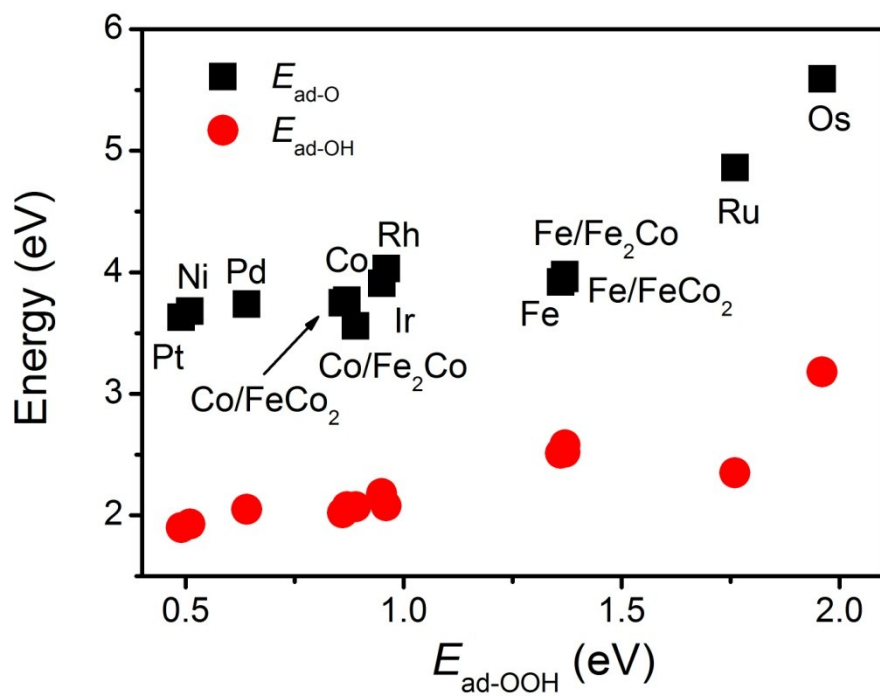


Fig. S8. Adsorption energies (E_{ad}) of O and OH plotted against the E_{ad} of OOH on $M_3(\text{THT})_2$ nanosheets.